INSTITUTE OF PHYSICS PUBLISHING NANOTECHNOLOGY
Nanotechnology **17** (2006) S121–S127 doi:10.1088/0957-4484/17/7/S04

Simulated measurement of small metal clusters by frequency-modulation non-contact atomic force microscopy

S C Fain Jr[1,5], C A Polwarth[1], S L Tait[1,6], C T Campbell[2] and R H French[3,4]

[1] Physics Department, University of Washington, Seattle, WA 98195-1560, USA
[2] Chemistry Department, University of Washington, Seattle, WA 98195-1700, USA
[3] Materials Science and Engineering, University of Pennsylvania, Philadelphia, PA 19104, USA
[4] DuPont Co. Central Research, Wilmington, DE 19880, USA

E-mail: fain@phys.washington.edu

Received 3 October 2005, in final form 7 November 2005
Published 10 March 2006
Online at stacks.iop.org/Nano/17/S121

Abstract
The apparent height and lateral extent of very small metallic clusters and particles adsorbed on flat substrates have been calculated for frequency-modulation non-contact atomic force microscopy (ncAFM). The ncAFM scanning tip was modelled as a Si sphere covered by 1 nm of SiO_2. This tip sphere of either 5 or 20 nm total radius (including an SiO_2 layer) is attached to a cantilever of spring constant $k = 40$ N m^{-1} and oscillated with a 10 nm amplitude. The tip was rastered across the centre of a single cluster of Pd atoms or a single Pd particle located on a flat continuum substrate of alumina or Pd. The clusters were one-atom-thick close-packed arrangements of 19 or 91 atoms (1.4 or 3.0 nm wide); the particles were continuum spheres of diameter 2.0 or 4.0 nm. The tip–substrate and tip–particle interactions were modelled with 6–12 Lennard-Jones potentials. The attractive interaction was taken to be the London–van der Waals dispersion interaction whose magnitude was estimated from Hamaker constants calculated from bulk optical constants of Si, SiO_2, Pd, and alumina. The repulsive interaction was determined from estimates of the atomic radii using densities of the bulk materials. These simulations show that the apparent heights of particles imaged by ncAFM range from just 12% of the actual height for the smallest Pd cluster on a Pd substrate to 95% of the actual height for the largest Pd particle on an alumina substrate. The apparent widths of the clusters were similar to those in contact AFM. These results show the most accurate height measurements occur when the lateral extent of the cluster or particle is comparable to or larger than the radius of the tip and when the Hamaker constant for the interaction of the tip with a cluster or particle is larger than that for the tip with the substrate.

1. Introduction

Future developments in nanotechnology may require accurate measurements of very small, atom-high particles on insulating surfaces. Frequency-modulation non-contact atomic force microscopy (ncAFM) has provided impressive atomic resolution on insulating surfaces [1–3], giving ncAFM great potential for detecting and measuring very small particles. Experiments for Pd clusters on α-alumina indicated that ncAFM with conventional Si tips was not detecting the smallest clusters and was incorrectly measuring the height of clusters

[5] Author to whom any correspondence should be addressed.
[6] Current address: Max Planck Institute for Solid State Research, Heisenbergstraße 1, D-70569 Stuttgart, Germany.

it did detect [4, 5]. The present work was carried out to estimate under what conditions ncAFM can be expected to correctly measure the height of small clusters on flat surfaces. The simulations are confined to Si tips represented as continuum spheres of radius 5 or 20 nm interacting with simple cluster or particle shapes. The tip–sample interactions are approximated by pairwise integrations of Lennard-Jones 6–12 atom–atom interactions (no electrostatic, magnetic, and chemical interactions). The model of a sphere to represent an extended tip has previously been shown to be appropriate for ncAFM [6]. The conical part of the tip remote from the spherical end of radius R_{tip} does contribute a significant portion of the total force when the end of the tip is at distances from the substrate comparable to or greater than R_{tip}. However, the integral over distance which determines the frequency shift in ncAFM is primarily determined by the forces at the closest approach distance (in the absence of electrostatic, magnetic, or other long-range forces) [6]. Two Pd cluster or particle shapes, each in two sizes, are considered: (a) one-atom-high close-packed (i.e., (111)-like) hexagonal clusters of either 19 or 91 atoms with widths of 1.4 or 3.0 nm, and (b) continuum spherical particles with diameters of either 2.0 and 4.0 nm. The substrate is represented as a semi-infinite continuum with properties chosen to represent α-alumina or Pd.

The electronics in ncAFM measure the resonant frequency f of the tip–cantilever system (tip) as it is forced to oscillate between a closest approach distance z (measured here from the edge of the substrate to the edge of the tip) and a distance $z + 2A$ from the edge of the substrate to the edge of the tip, where A is the oscillation amplitude of the tip. For ncAFM topography measurements, a feedback circuit adjusts the tip–substrate closest approach distance z to maintain a constant frequency shift $\Delta f = f - f_0$, where f_0 is the resonant frequency when the tip is far away from the substrate. Typical ncAFM measurements are made in the region where the tip–sample interaction is attractive ('attractive force' region). In order for the ncAFM distance feedback circuit to function stably, the motion of the ncAFM tip must be in a region where the frequency shift Δf changes monotonically with z (Δf increases in magnitude (becomes more negative) with decreasing z).

Our calculations indicate that the heights of clusters are seriously underestimated (as small as 12% of the actual height) when the tip diameter is large compared with the lateral extent of the particle, consistent with recent experimental observations [4, 5]. The errors are reduced somewhat for clusters with Hamaker constants higher than the substrate. The attractive van der Waals interaction has been previously shown to cause ncAFM errors in topography measurements near steps [7] as well as in the difference in the apparent height of adsorbed molecules [8].

2. Simulation parameters and geometries

2.1. Potentials

The calculations used Lennard-Jones 6–12 atom–atom pair potentials V_{1j} to represent the effective interactions of atoms in the tip (subscript 1) with atoms of Pd (subscript 2) or atoms of alumina (subscript 3).

$$V_{1j}(r) = 4\varepsilon_{1j}\left[\left(\frac{\sigma_{1j}}{r_{1j}}\right)^{12} - \left(\frac{\sigma_{1j}}{r_{1j}}\right)^{6}\right] \tag{1}$$

where r_{1j} is the distance between the centres of the two atoms, and σ_{1j} and ε_{1j} are species-dependent constants determined as indicated below. Such a potential has been used in a number of published ncAFM simulations, such as for the ncAFM interaction between one Si tip atom and one layer of xenon atoms [9, 10]. Summation of this pairwise potential over the atoms in two bodies yields the net van der Waals interaction between those bodies [11–13]. Exact analytical integrals of this interaction [5] were used instead of short-distance approximations [12]. This potential was integrated over a continuum sphere used to model the AFM tip and then either summed over Pd atoms in the one-atom-thick clusters or integrated over Pd atoms in spherical Pd clusters. This potential was also evaluated for the interaction between a spherical tip and a semi-infinite slab of either Pd or alumina, which is used to model AFM tip–substrate interactions.

2.2. Lennard-Jones parameters

Hamaker constants were used to determine the attractive (London dispersion) component of the Lennard-Jones equation (1). These were obtained from full-spectrum calculations [14] using experimentally measured bulk optical constants for Si and SiO_2 [15], Pd [16], and alumina [14], and are listed in table 1. These Hamaker constant calculations are based on Lifshitz quantum electrodynamics theory [17], taking into consideration both the effects of retardation and an arbitrary number of materials layers in the configuration, and have been applied to sub-nanometre materials configurations previously [18]. The subscript v in H_{ivj} represents the vacuum layer which is taken as the variational layer in each of these free energy calculations of the London dispersion interaction. The Hamaker constants for the tip–cluster interaction (H_{1v2}) and the tip–substrate interaction (H_{1v2} for Pd substrate or H_{1v3} for Al_2O_3 substrate) given in table 1 were calculated for two different materials configurations of the tip, either a bare Si tip, or a tip on which a 1 nm thick layer of SiO_2 had formed. The apparent heights of the clusters studied turned out to be dependent on the ratio of the tip–cluster Hamaker constant to the tip–substrate Hamaker constant, which we define as $a = H_{1v2}/H_{1vs}$, where the subscript s refers to the substrate which is either Pd ($j = 2$) or Al_2O_3 ($j = 3$). This ratio for Pd on Al_2O_3 is not strongly affected by a SiO_2 layer on the Si.

The attractive part of the van der Waals interaction was then determined from bulk particle densities ρ_i and from the Hamaker constants by

$$4\varepsilon_{1j}\sigma_{1j}^6 = \frac{H_{1vj}}{\rho_1\rho_j\pi^2}, \tag{2}$$

where the value of σ_{1j} was obtained from

$$\sigma_{1j} = (\sigma_{11} + \sigma_{jj})/2. \tag{3}$$

When both tip and substrate or tip and particle are treated as continua, the sphere-to-plane or sphere-to-sphere integral involves the same product $\rho_1\rho_j$ as equation (2) and one can

Table 1. Volume densities ρ_i, Hamaker constants (H_{ivj}) where v corresponds to vacuum (Vac.), and van der Waals parameters σ_{ij} and ε_{ij}.

Materials and configuration	ρ_i (10^{28} m^{-3})	$H_{ivj}(zJ)$[b]	H_{ivj} ratio[h]	σ_{ij} (nm)	ε_{ij} (eV)
Si|Vac.|Si	5.00	$H_{1v1} = 212$[c]		0.280	2.66×10^{-2}
Pd|Vac.|Pd	6.80	$H_{2v2} = 375$[d]		0.252	5.24×10^{-2}
Al_2O_3|Vac.|Al_2O_3	7.07[a]	$H_{3v3} = 168$[e]		0.249	2.23×10^{-2}
Si|Vac.|Pd		$H_{1v2} = 271$[f]			
Si|Vac.|Al_2O_3		$H_{1v3} = 175$[f]			
H(Si|Vac.|Pd)/H(Si|Vac.|Al_2O_3)			$a = 1.55$		
Si|1 nm SiO_2|Vac.|Pd		$H_{1v2} = 165$[g]		0.266	2.17×10^{-2}
Si|1 nm SiO_2|Vac.|Al_2O_3		$H_{1v3} = 110$[g]		0.264	1.46×10^{-2}
H(Si|1 nm SiO_2|Vac.|Pd)/H(Si|1 nm SiO_2|Vac.|Al_2O_3)			$a = 1.50$		
H(Si|1 nm SiO_2|Vac.|Pd)/H(Si|1 nm SiO_2|Vac.|Pd)			$a = 1.00$		

[a] Assuming 3 O quasiatoms per Al_2O_3.
[b] 1 zeptojoule (zJ) $= 10^{-21}$ J.
[c] Calculated from optical constants in French *et al* [15] for a vacuum gap less than 1 nm.
[d] Calculated from optical constants in Palik [16] for a vacuum gap less than 1 nm.
[e] Calculated from optical constants very similar to those used in French [14] for a vacuum gap less than 1 nm.
[f] Calculated for a vacuum gap less than 1 nm.
[g] Calculated for a vacuum gap less than 1 nm when there is a 1 nm thick SiO_2 layer on the Si surface.
[h] The tip–surface H_{ivj} ratio is defined as $a = H_{1v2}/H_{1vs}$ where s refers to the substrate, which is either Pd ($j = 2$) or Al_2O_3 ($j = 3$).

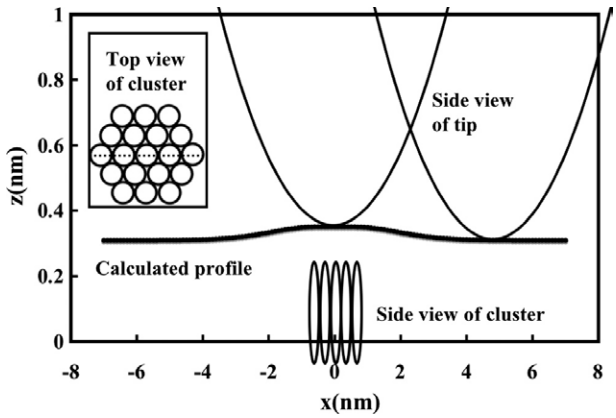

Figure 1. Calculated topography profile z versus x for an $R_{tip} = 20$ nm tip scanned across a 19-atom Pd cluster on an Al_2O_3 continuum substrate at $z < 0$. The cluster is shown in top view in the inset at upper left; the dotted line is the path of the tip for the profiles shown for clusters. Outside of the inset, the vertical z scale is exaggerated by a factor of 10 relative to the horizontal x scale. The centre of the Pd atoms is located at 0.112 nm (0.5 of the bulk Pd(111) interplanar spacing) above the edge of the continuum representation of Al_2O_3. The diameter of the Pd atoms shown is the same as the lateral spacing of the Pd atoms, which is assumed to be the bulk nearest-neighbour spacing of 0.275 nm. All calculations assumed a cantilever spring constant of $k = 40$ N m^{-1} and an oscillation amplitude of $A = 10$ nm.

then show that the value of σ_{1j} affects only the repulsive part of the interaction potential. For simplicity in calculation, we assumed arbitrarily that the tip, Pd, and alumina are all face-centred-cubic (fcc) solids with the number density of atoms per unit volume ρ_i. The parameters σ_{ii} were determined from the nearest-neighbour distance (d_{ii}) from the relationship for a zero temperature fcc solid bound by the 6–12 potential [19]

$$\sigma_{ii} = d_{ii}/1.09. \tag{4}$$

The tip density ρ_1 was taken to be that of bulk Si. The alumina solid was modelled as a uniform fcc solid of three quasiatoms per Al_2O_3 unit. The 'atomic radius' of these quasiatoms was determined by their number density in Al_2O_3. (This is assumed to approximately represent the finding of Soares *et al* [20] that the Al–O bonds of the surface Al atoms are almost parallel to the surface atoms in the top layers of alumina.) Table 1 shows the values of the parameters. For this choice of quasiatom for Al_2O_3 the number density per unit volume is very similar for Pd and Al_2O_3. Results not shown here indicated that the choice of σ_{1j} does affect the frequencies, but it does not significantly affect the apparent heights or widths of the clusters.

2.3. Geometries

In order to locate the Pd atoms relative to the substrate, we assumed that the edge of the continuum substrate is located at one half the bulk (111) interplanar spacing from the centre of the atoms in the outermost layer of the substrate (0.112 nm for Pd). Figure 1 shows the geometry of the smallest cluster and the end of a 20 nm radius Si tip along with an apparent height profile to be discussed below. Except for the inset that shows a top view, the vertical scale on this figure has been exaggerated by a factor of 10. The diameter of the Pd atoms shown is identical to the nearest-neighbour spacing (0.275 nm) of bulk Pd. The spherical Pd particles were positioned so their edge contacted the edge of the continuum substrate.

3. Profiles derived from simulations of frequency shift

Simulating the topography profile (z as a function of lateral position x) requires calculating the frequency shift as a function of z (vertical axis in figure 1) for each lateral position x (i.e., at a number of positions along the horizontal axis in figure 1). Calculations are presented here for lateral positions x along a symmetry axis of a Pd cluster (shown as a dotted line in the inset of figure 1 for the 19-atom cluster) or along the centre-line of a Pd spherical particle

Tip–surface forces in the z-direction were calculated from a numerical derivative of the total potential at instantaneous

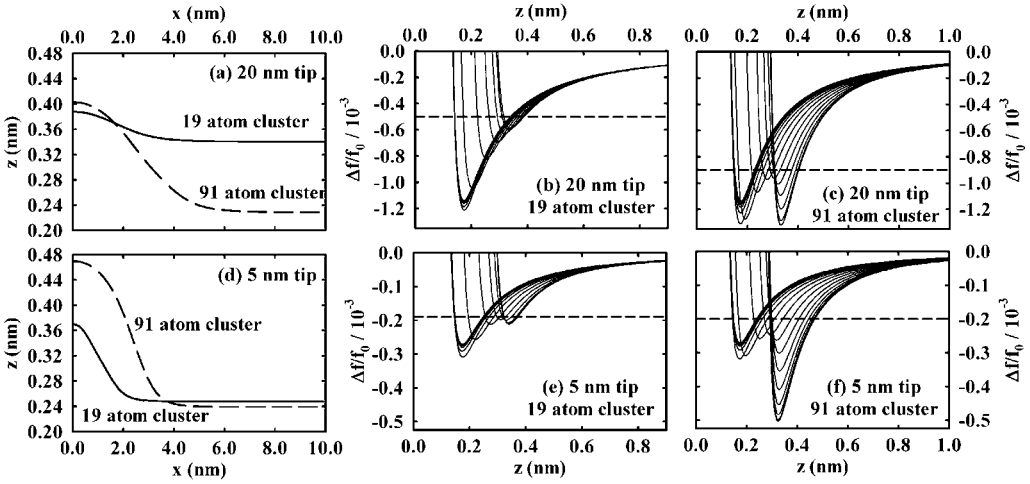

Figure 2. Calculated frequency shifts $\Delta f/f_0$ versus z (b), (c), (e), (f) and topography profiles z versus x ((a), (d)) for 20 and 5 nm radius silicon tips scanning over 19- and 91-atom clusters of Pd atoms located near the edge of an Al_2O_3 continuum as shown in figure 1. The frequency shift $\Delta f/f_0$ is plotted as a function of the closest approach distance z between the edge of the tip and the edge of the substrate and is shown for lateral positions x starting over the centre of the cluster (the curve with the most negative minimum near $z = 0.34$ nm) and moving by intervals of 0.3 nm for $R_{tip} = 5$ nm ((e), (f)) or 0.5 nm for $R_{tip} = 20$ nm ((b), (c)) laterally away from the centre until only the substrate contributes (the curve with least negative extremum near $z = 0.17$ nm). Horizontal dashed lines indicate the frequency shifts $\Delta f/f_0$ used for the lateral profiles: -5.0×10^{-4} (b), -9.0×10^{-4} (c), -1.9×10^{-4} (e), and -2.0×10^{-4} (f).

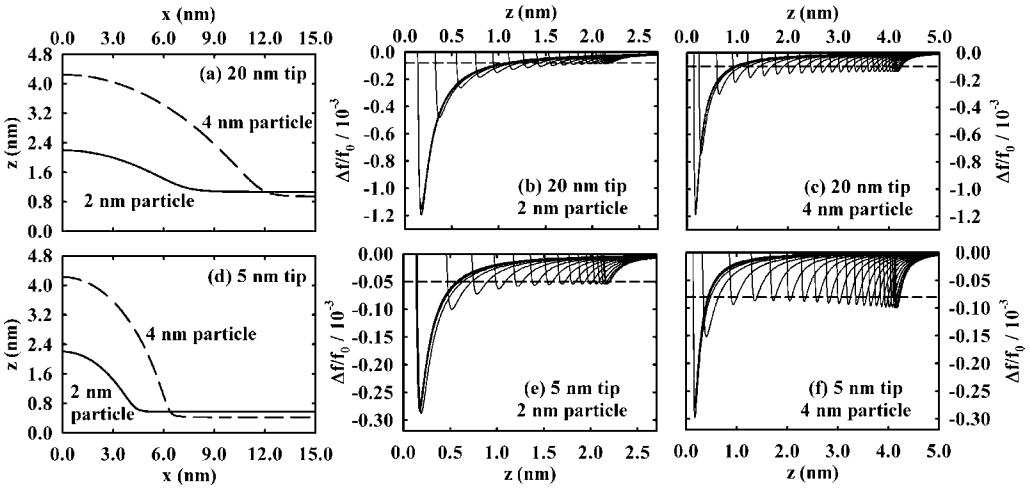

Figure 3. Calculated frequency shifts $\Delta f/f_0$ versus z (b), (c), (e), (f) and topography profiles z versus x ((a), (d)) for 20 and 5 nm radius silicon tips scanning over 2 and 4 nm diameter continuum Pd particles just contacting the edge of an Al_2O_3 continuum. The frequency shift $\Delta f/f_0$ is plotted as a function of the closest approach distance z between the edge of the tip and the edge of the substrate and is shown for lateral positions starting over the centre of the cluster (the curve with the minimum at the largest z) and moving by intervals of 0.3 nm for $R_{tip} = 5$ nm ((e), (f)) or 0.5 nm for $R_{tip} = 20$ nm ((b), (c)) laterally away from the centre until only the substrate contributes (the curve with least negative extremum near $z = 0.17$ nm). Horizontal dashed lines indicate the frequency shifts $\Delta f/f_0$ used for the lateral profiles: -0.8×10^{-4} (b), -1.0×10^{-4} (c), -5.0×10^{-5} (e), and -8.0×10^{-5} (f).

tip–surface distance intervals of 0.01 nm. The frequency shifts $\Delta f/f_0$ were then calculated from the tip–surface forces using a discretized method described by Giessibl [21]. Note that the resonant frequency shifts are only affected by the forces perpendicular to the surface. The results presented here are for tip oscillation amplitude $A = 10$ nm and a spring constant $k = 40$ N m^{-1}. Calculations not shown here indicated that the topography profiles were approximately independent of amplitude for $A > 0.1$ nm.

Examples of the frequency shifts $\Delta f/f_0$ plotted versus the nearest approach distance z are shown in figures 2(b), (c), (e), (f) for one-atom-thick Pd atom clusters and in figures 3(b), (c), (e), (f) for spherical Pd particles. In each of these figures there are several $\Delta f/f_0$ versus z curves, corresponding to different lateral positions x of the tip across the particle. The frequency shifts were calculated at several horizontal positions along a symmetry axis of the cluster or particle, starting over the centre (e.g., the curve with the most negative minimum near $z = 0.34$ nm in figures 2(b), (c), (e), (f) or near $z = 2$ and 4 nm in figures 3(b), (e) and (c), (f), respectively) and moving by intervals of 0.5 nm for $R_{tip} = 20$ nm (panels (b), (c) in figures 2 and 3) or 0.3 nm for

$R_{tip} = 5$ nm (panels (e), (f) in figures 2 and 3) laterally away from the centre until the x position is far enough from the cluster or particle that only the substrate force remains (the curve in each panel with the least negative minima located near $z = 0.17$ nm). The frequency shifts are more negative for the larger tip and for the larger cluster or particle where there is a much greater tip interaction.

As the tip moves laterally away from the centre of the cluster (x increasing from 0) and thus interacts less strongly with the cluster, the negative extremum of the frequency shift for figures 2(c), (e), (f) and figures 3(c), (f) becomes more positive, with the largest effect for the $R_{tip} = 20$ nm tip in figures 2 and 3. As the x position of the tip subsequently moves further away from the centre of the cluster, the negative extremum starts to become more negative and moves to smaller z as the tip is able to approach closer to the substrate. The negative extremum becomes more negative than for the bare substrate at a point where part of the tip is attracted to the cluster and part is attracted to the substrate, with the largest effect for the clusters in figure 2.

The line profiles in figures 2(a), (d) and 3(a), (d) were determined from the largest z position (as the tip approaches the surface) for each position x at which the frequency shift $\Delta f/f_0$ was equal to the setpoint shown by horizontal dashed lines in figures 2(b), (c), (e), (f) and in figures 3(b), (c), (e), (f). In other words, each data point along a profile curve $z(x)$ is obtained from the $\Delta f/f_0$ versus z curve calculated at that value of x by finding the largest z where the frequency shift setpoint condition is met. These profiles are what would be obtained from an ncAFM image made with close to optimal feedback conditions. Accurate measurement of the heights of small clusters or particles requires that the $\Delta f/f_0$ setpoint (used for topography feedback in ncAFM) be as negative as possible consistent with a monotonic increase in frequency shift with increasing distance z between the closest approach of tip and the sample for every x, y position included in a scan. In other words, a more negative frequency shift setpoint allows a more accurate measure of true nanoparticle height (up to a point, as discussed below). This is illustrated by an example in figure 4 where the change in apparent height as a function of the frequency setpoint is shown for a 91-atom cluster of Pd on Al_2O_3 interacting with an $R_{tip} = 20$ nm Si tip.

However, if the frequency shift setpoint is too negative the topography feedback will become unstable in regions of the sample where the frequency shift cannot reach the setpoint (i.e., the $\Delta f/f_0$ versus z curve minimum value is less negative than the setpoint value). In all the examples shown in figures 2 and 3, the setpoint must be at a less negative frequency than the most negative frequency over the bare substrate. In figures 2(c), (e), (f) and 3(e), (f), the setpoint must also be at a less negative frequency than the most negative frequency over the centre of the cluster or particle in order to satisfy the stability criterion for every x, y position over the cluster. Note that for a less negative frequency shift setpoint, the apparent height of the particles is smaller, as illustrated in figure 4.

Figures 5 and 6 compare the topography profiles for Pd on Al_2O_3 shown in figures 2 and 3 (dotted line, shifted to give zero height over the substrate) with the profiles that would result from a freely sliding contact between the end of the spherical tip and the cluster or particle (solid line). For the sliding contact

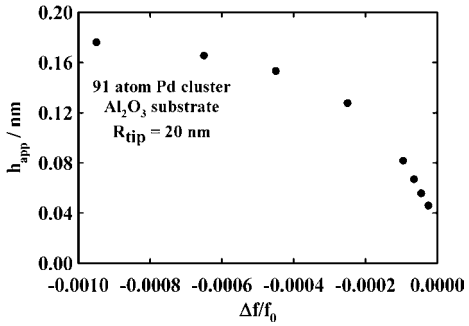

Figure 4. The apparent height h_{app} of a 91-atom cluster of Pd on Al_2O_3 interacting with a 20 nm Si tip shown as a function of the frequency shift setpoint $\Delta f/f_0$. Note that the apparent height becomes larger as the setpoint is made more negative. At setpoints more negative than shown here, the feedback becomes unstable, as discussed in the text.

profiles, we have somewhat arbitrarily assumed (1) that the contact point between the tip and the Pd atoms in the clusters occurs at the edge of the Pd atoms described in figure 1, and (2) that the contact point of the tip with either the continuum spherical Pd particles or the continuum planar substrate occurs at the edges of the continua. Using these criteria, the profiles at the setpoints used for figures 2 and 3 (dotted lines in figures 5 and 6) give an apparent height of each cluster or particle that is less than the true height in each case. Profiles are also shown by dashed lines for a less negative frequency shift setpoint (approximately 1/10 the magnitude of the value used in figures 2 and 3) where the apparent height of the particles is even smaller, as expected from figure 4. These dashed lines in figures 5 and 6 illustrate that the underestimation of actual particle sizes by ncAFM becomes more extreme when the ncAFM frequency shift setpoint is much less negative than the close optimum value used for the dotted lines. This will almost always be the case in actual ncAFM experiments, as the optimum setpoint value can only be found in experiment by gradually increasing the magnitude of the setpoint until the scanning feedback becomes unstable. Thus the height values calculated in this work should be taken as indicating upper limits on the actual heights one would obtain in actual experiments on metal clusters.

Table 2 summarizes the ratio between the apparent height and actual height for both Pd clusters and particles on an Al_2O_3 substrate (where the ratio of Hamaker constants defined earlier is $a = 1.50$ for figures 2 and 3) and for similar calculations for Pd on Pd (where $a = 1.00$). It is evident from this table that the most accurate height measurements occur when the lateral extent of the cluster or particle is comparable to or larger than the radius of the tip and when the Hamaker constant for the interaction of the tip with a cluster or particle is larger than that for the tip with the substrate.

Widths of profiles in ncAFM are typically measured from a point where the height increases by a certain amount above the value far away from the cluster, such as 0.03 nm for the experimental results of Tait *et al* [4]. Figures 5 and 6 show that the apparent widths of the profiles are approximately the same for the setpoints used for figures 2 and 3 (dotted lines) as those of a sliding contact (solid lines). The widths of profiles

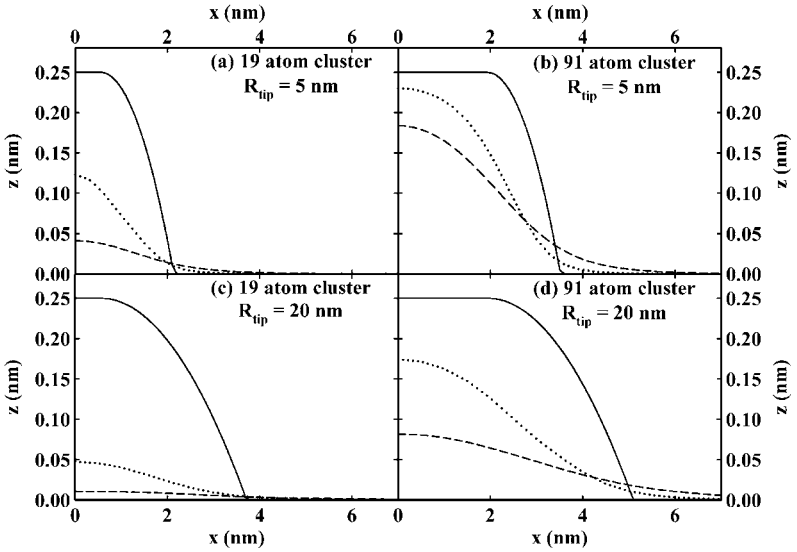

Figure 5. Comparison of topography profiles for Pd clusters on Al_2O_3 for a sliding contact between tip and surface (solid lines) with profiles for the frequency setpoints used in figure 2 (dotted lines) and with profiles for frequency setpoint about a factor of 10 less in magnitude than those used for figure 2 (dashed lines). The Pd clusters with 19 atoms (panels (a) and (c)) and 91 atoms (panels (b) and (d)) are 1.4 and 3.0 nm in diameter, respectively. The apparent widths are greater than the actual widths due to the finite size of the tips: 5 nm for (a), (b) or 20 nm for (c), (d). Note that the apparent heights approach the real heights as the lateral extent of the clusters becomes comparable to or larger than the tip radius.

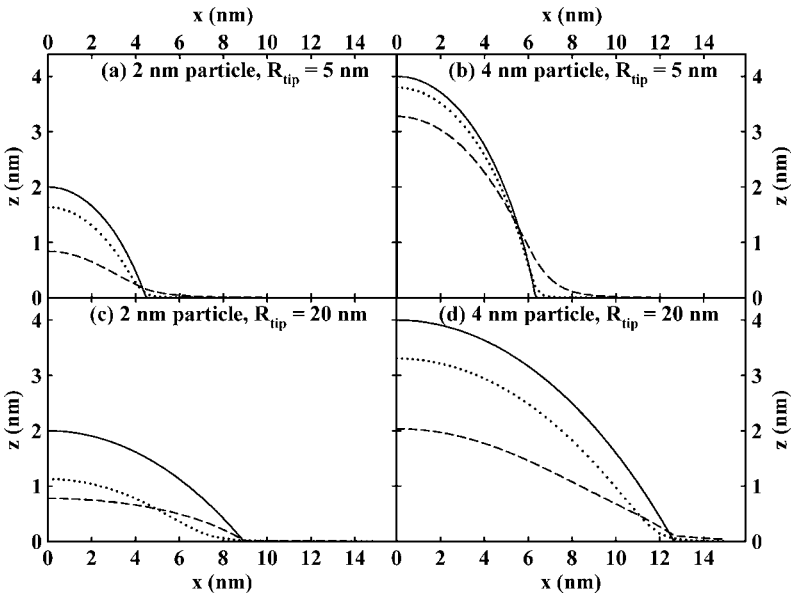

Figure 6. Comparison of topography profiles for Pd particles on Al_2O_3 for a sliding contact between tip and surface (solid lines) with profiles for the frequency setpoints used in figure 3 (dotted lines) and with profiles for frequency setpoint about a factor of 10 less in magnitude than those used for figure 3 (dashed lines). The Pd particles are 2 nm (panels (a) and (c)) and 4 nm (panels (b) and (d)) in diameter. The apparent widths are greater than the actual widths due to the finite size of the tips: 5 nm for ((a), (b)) or 20 nm for ((c), (d)). Note that the apparent heights approach the real heights as the lateral extent of the clusters becomes comparable to or larger than the tip radius.

at the smallest setpoints shown (dashed lines) are a bit wider than for the values used for figures 2 and 3 (dotted lines).

A surprising feature of the present calculations where the clusters are represented by atoms is that, for the 5 nm radius tip interacting with a 91-atom Pd cluster on a Pd continuum substrate, the frequency shift similar to that shown in figure 2(f) is more negative on the cluster than over the substrate. Additional calculations show that the frequency shift over the centre of a one-layer-high atom cluster monotonically increases as the number of atoms in the cluster increases and that a complete Pd layer represented as a plane of atoms above a continuum Pd substrate has a more negative frequency shift than a bare Pd substrate represented as a continuum. This seems unrealistic because adding a complete layer to a real solid will change only the absolute location, but not the depth of the extrema in potentials, forces, and frequency shifts. The most likely explanation is that mixing an atom-by-atom model of a cluster with continuum models of the tip and substrate is

Table 2. Ratio of apparent height to actual height for two tip radii R_{tip} and two different values of $a = H_{1v2}/H_{1vs}$, where s refers to the substrate, which is either Pd ($j = 2$, $a = 1.0$) or Al_2O_3 ($j = 3$, $a = 1.5$). Note that the ratio of apparent height to actual height approaches 1.00 as the lateral extent of the clusters becomes comparable to or larger than the tip radius R_{tip} and as the Hamaker constant for the interaction of the tip with a cluster or particle becomes larger than that for the tip with the substrate.

Lateral diameter	$R = 20$ nm $a = 1.0$	$R = 20$ nm $a = 1.5$	$R = 5$ nm $a = 1.0$	$R = 5$ nm $a = 1.5$
1.4 nm cluster (19 atoms)	0.12	0.19	0.37	0.49
2.0 nm spherical particle	0.44	0.57	0.73	0.82
3.0 nm cluster (91 atoms)	0.56	0.70	0.77	0.92
4.0 nm spherical particle	0.78	0.83	0.92	0.95

not a completely accurate representation for the small distances shown here. A similar mix of continuum and atomistic models has been used by other investigators in ncAFM calculations without comments about possible difficulties [1, 8, 22]. While representing the substrate as a series of planes may provide somewhat more accurate results than the continuum model, the qualitative features of the results presented here are not expected to change.

4. Summary

Simulation of the topography profiles in ncAFM obtained for very small clusters or particles on flat surfaces imaged by spherical tips shows that the apparent heights produced by the ncAFM technique underestimate the true particle height by as much as 80%. The apparent heights approach the real heights as the lateral extent of the clusters or particles becomes comparable to or larger than the tip radius and as the Hamaker constant for the interaction of the tip with a cluster or particle becomes larger than that for the tip with the substrate. In addition the apparent widths of the clusters and particles for the topography profiles are close to those for a sliding contact between tip and substrate

The present calculations form a basis for more detailed future calculations that would include effects known to be important for atomic resolution on flat surfaces, such as short-range chemical forces, distortion of the tip, cluster, or substrate due to short-range forces, and nanotips that protrude from the end of spherical tips [1, 6, 23]. In the presence of nanotips, Barth and co-workers [24] have shown both experimentally and theoretically that the lateral extent of flat-topped clusters such as the 19- and 91-atom clusters shown here is more accurately measured by a constant-height mode, where the feedback on the frequency shift is too slow to respond as the tip is scanned over a cluster. However, the height of a cluster must at present be estimated from measurements with feedback on frequency shift if individual atomic layers cannot be resolved.

Acknowledgments

The authors gratefully acknowledge support from NSF DMII-0508216 (SCF), UW NASA Space Grant and UW Mary Gates Fellowship (CAP), Joint Institute for Nanoscience funded by UW and Pacific Northwest National Laboratory (operated by Battelle for the US Department of Energy) (SLT), DOE OBES Office of Chemical Sciences (SLT and CTC), and NSF DMR-0010062 in cooperation with EU Commission Contract G5RD-CT-2001-00586 (RHF). In addition, SCF acknowledges useful discussions about this subject with J M K Donev, B R Long, R K Bollinger, Q M Yu, J J Rehr, C Barth, G Radu, and L Bruch.

References

[1] Barth C, Foster A S, Reichling M and Shluger A L 2001 *J. Phys.: Condens. Matter* **13** 2061
[2] Morita S, Wiesendanger R and Meyer E 2002 *Noncontact Atomic Force Microscopy* (*NanoScience and Technology*) ed P Avouris, K von Klitzing, H Sakaki and R Wiesendanger (Berlin: Springer)
[3] Giessibl F J 2003 *Rev. Mod. Phys.* **75** 949
[4] Tait S L, Ngo L T, Yu Q M, Fain S C and Campbell C T 2005 *J. Chem. Phys.* **122** 64712
[5] Tait S L 2005 *PhD Dissertation* University of Washington, Seattle
[6] Guggisberg M, Bammerlin M, Loppacher C, Pfeiffer O, Abdurixit A, Barwich V, Bennewitz R, Baratoff A, Meyer E and Guntherodt H J 2000 *Phys. Rev.* B **61** 11151
[7] Guggisberg M, Bammerlin M, Baratoff A, Luthi R, Loppacher C, Battiston F M, Lu J, Bennewitz R, Meyer E and Guntherodt H J 2000 *Surf. Sci.* **461** 255
[8] Sasahara A, Uetsuka H, Ishibashi T and Onishi H 2002 *Appl. Surf. Sci.* **188** 265
[9] Giessibl F J and Bielefeldt H 2000 *Phys. Rev.* B **61** 9968
[10] Holscher H, Allers W, Schwarz U D, Schwarz A and Wiesendanger R 2001 *Appl. Phys.* A **72** S35
[11] Hamaker H C 1937 *Physica* **4** 1058
[12] Israelachvili J N 1992 *Intermolecular and Surface Forces* (London: Academic)
[13] Argento C and French R H 1996 *J. Appl. Phys.* **80** 6081
[14] French R H 2000 *J. Am. Ceram. Soc.* **83** 2117
[15] French R H, Cannon R M, Denoyer L K and Chiang Y M 1995 *Solid State Ion.* **75** 13
[16] Palik E D 1991 *Handbook of Optical Constants of Solids* vol 2 (Boston, MA: Academic)
[17] Lifshitz E M 1956 *Sov. Phys.* **2** 73
[18] van Benthem K, Tan G L, DeNoyer L K, French R H and Ruhle M 2004 *Phys. Rev. Lett.* **93** 227201
[19] Kittel C 2005 *Introduction to Solid State Physics* (Hoboken, NJ: Wiley)
[20] Soares E A, Van Hove M A, Walters C F and McCarty K F 2002 *Phys. Rev.* B **65** 195405
[21] Giessibl F J 2001 *Appl. Phys. Lett.* **78** 123
[22] Garcia R and Perez R 2002 *Surf. Sci. Rep.* **47** 197
[23] Hofer W A, Foster A S and Shluger A L 2003 *Rev. Mod. Phys.* **75** 1287
[24] Barth C, Pakarinen O H, Foster A S and Henry C R 2006 *Nanotechnology* **17** S128–36